Eur. Phys. J. D **6**, 333–341 (1999)

THE EUROPEAN PHYSICAL JOURNAL D

EDP Sciences

LiAr, LiKr and LiXe excimers: Photochemical formation of the $3^2\Sigma^+$-$1^2\Sigma^+$ bands

D. Azinović[1,a], S. Milošević[1], G. Pichler[1], M.C. van Hemert[2], and R. Düren[3]

[1] Institute of Physics, P. O. Box 304, Zagreb, Croatia
[2] Department of Chemistry, Gorleaus Laboratory, University of Leiden, P. O. Box 9502, 2300 RA Leiden, The Netherlands
[3] Max-Planck-Institut für Strömungsforschung, 37018-Göttingen, Germany

Received: 2 October 1998 / Received in final form: 25 January 1999

Abstract. We investigated the photochemical formation of lithium–rare-gas excimers in the $3^2\Sigma^+$ state through the reaction of $Li_2(2(C)^1\Pi_u)$ and the ground-state rare-gas atom. Lithium–rare-gas vapor mixture was prepared in the heat-pipe oven. We populated the $2(C)^1\Pi_u$ state of the Li_2 molecule using the XeCl excimer laser wavelength at 308 nm or the PTP dye laser wavelength at about 335 nm. The $3^2\Sigma^+$-$1^2\Sigma^+$ transitions were observed with peaks at 414, 420 and 435 nm for LiAr, LiKr and LiXe, respectively. We estimated thermally averaged rate constants for these photochemical reactions, which are $(2.3\pm1.1)\cdot10^{-10}\mathrm{cm}^3\mathrm{s}^{-1}$ for LiAr, $(6.9\pm3.2)\cdot10^{-10}\mathrm{cm}^3\mathrm{s}^{-1}$ for LiKr and $(19\pm9)\cdot10^{-10}\mathrm{cm}^3\mathrm{s}^{-1}$ for LiXe. *Ab initio* potential-energy curves and transition dipole moments for LiKr were calculated applying the SCF MRDCI method. Available data for the LiAr and LiKr excimers are presented, including potential-energy curves, electronic transition dipole moments, and spectroscopic constants. Possible photochemical formation of these molecules in the excited states is discussed. We performed the quantum-mechanical spectral simulations of the LiAr and LiKr $3^2\Sigma^+$-$1^2\Sigma^+$ transitions, using *ab initio* potential-energy curves.

PACS. 33.20.Kf Visible spectra – 82.20.Pm Rate constants, reaction cross-section and activation energies – 34.20.Cf Interatomic potentials and forces

1 Introduction

The alkali–rare-gas (RG) molecular bands have been extensively studied for the past thirty years which were systematized in the review paper published by Rostas [1]. Alkali-RG $3^2\Sigma^+$-$1^2\Sigma^+$ transitions, investigated by applying the laser induced fluorescence method or electric discharge, were reported by Tam *et al.* [2–4], Webster and Rostas [5] and Wang and Havey [6].

In our previous work we studied the photochemical formation of the $2^2\Pi$-$1^2\Sigma^+$ excimer bands of LiZn [7], LiCd [8], NaZn [9]. The IIB atoms and rare gases have a closed outer electronic shell. The structure and spectra of alkali-IIB and alkali–rare-gas molecules appear to be similar and one can compare the features of those two groups of molecules. The potential well for the $2^2\Pi$ state of alkali-IIB excimers is deeper than the $3^2\Sigma^+$ state and the wells overlap partly. In contrast, the wells of the alkali-RG $3^2\Sigma^+$ and $2^2\Pi$ states do not overlap and it is possible to study transitions from these states separately. After our investigation of alkali-IIB excimers, we expected to observe the LiRG produced in a similar photochemical reaction. Tam *et al.* [3] were the first to observe photochemically produced alkali-RG bands. They excited the K_2 $2^1\Pi_u$ state by using the argon-ion laser line at 457.9 nm, which in collisions with RG produced the excited KRG excimer and one free potassium atom. Photochemical formation of the LiRG $3^2\Sigma^+$ state has not been investigated so far. The $1^2\Pi$ state of LiAr was photochemically formed in reactive collisions of the $Li_2(1(A)^1\Sigma_u^+)$, excited by a HeNe laser at a wavelength of 632.8 nm, and Ar [10].

The potential-energy curves of alkali-RG were calculated by Pascale and Vandeplanque using pseudopotential method [11]. *Ab initio* calculations of the potential-energy curves for LiRG are available for LiHe [12] and LiAr [13, 14]. Ground-state potentials were determined experimentally by Buck and Pauly [15] and recently by Brühl and Zimmermann [16] for LiAr, and by Auerbach [17] for LiKr and LiXe. The first excited $1^2\Pi$ states of LiAr and LiKr were published by Scheps *et al.* [18].

This paper is organized as follows. In Section 2 we present the experiment. The experimental results (Sect. 3) are given separately for XeCl excimer laser excitation, where we give the cross-section measurements for photochemical formation of LiRG relative to the collisional energy transfer of Li_2^*+Li system, and PTP dye laser excitation. In Section 4 we present results of the *ab initio* calculation of the LiKr potential-energy curves and transition dipole moments. In Section 5, the spectral simulation are performed using the *ab initio* potential-energy curves

[a] e-mail: azinovic@ifs.hr

for LiAr (Refs. [13,14]) and LiKr (this paper). In Section 6 we discuss the possibilities for photochemical formation of LiAr* and LiKr*, compare the experimental results with the simulations and estimate uncertainties in theoretical potential-energy curves and experimental rate constants for photochemical reactions. Conclusions are given in Section 7.

2 Experiment

The experimental arrangement is the same as in our previous paper [7]. The mixture of lithium, lithium dimer and rare gas was prepared in a crossed heat-pipe oven. The lithium vapor pressure was varied in the range from 5 to 20 Torr and rare-gas pressure in the range from 5 to 700 Torr. The temperature for the above-mentioned range of lithium pressures was varied from 900 K to 1150 K. When lithium vapor pressure was equal to the rare-gas pressure the heat-pipe oven was operating in the heat-pipe mode for lithium. In that case the mixing with rare gas in the central part of the heat-pipe oven was negligible and pure lithium and lithium dimer spectra were observed. For the observation of LiRG bands it was necessary to have the RG pressure higher than 30 Torr. The preparation of electronically excited Li_2 molecules in specific rovibrational levels of the $2(C)^1\Pi_u$ state is achieved by means of the pulsed XeCl excimer laser lines at 308 nm (LPX 105E) or using a pulsed dye laser (LPD 3002) working with PTP dye (range: 330-350 nm). The horizontal laser induced fluorescence was rotated by a Dove prism and focused to the vertical entrance slit of the monochromator. The resolution of the system was about 0.1 nm. The signal from the photomultiplier with S20 cathode was averaged by a boxcar averager (PARC M162 and M164). The analog output from the boxcar was digitized by an A/D converter and fed to a laboratory computer. The spectral response of the system was determined by means of a calibrated tungsten-ribbon lamp and was found constant in the region of interest (violet spectral region).

3 Results

3.1 XeCl excimer laser excitation

The XeCl excimer laser lines at 308 nm excite simultaneously the $v' = 13$, $J' = 6$ and the $v' = 19$, $J' = 24$ rovibrational levels in the $Li_2\, 2(C)^1\Pi_u$ state with the excitation energies of 24897.07 cm^{-1} and 26260.72 cm^{-1}, respectively. The 308 nm laser line should also excite energy levels above the potential barrier of the double-minimum $2^1\Sigma_u^+$ state, but they cannot be clearly identified since the spectroscopic constants for the rovibrational levels above the barrier are not well known. Identification of these transitions also requires a better spectral resolution. The $3^2\Sigma^+$ state of the lithium–rare-gas excimer is populated in the photochemical process, given by

$$Li_2(2(C)^1\Pi_u) + RG \rightarrow LiRG(3^2\Sigma^+) + Li\,. \qquad (1)$$

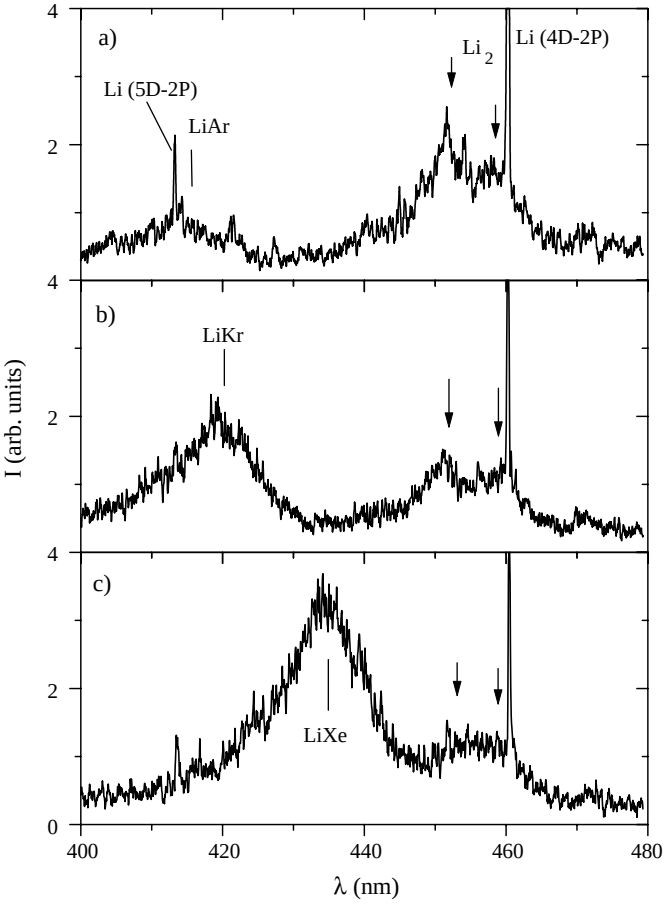

Fig. 1. a) The LiAr excimer band at 414 nm. Argon pressure is 150 Torr and the temperature 1161 K. b) The LiKr excimer band is at 420 nm. Krypton pressure is 300 Torr and T =1161 K. c) The LiXe excimer band is at 435 nm. Xenon pressure is 200 Torr and T =1161 K. The Li–rare-gas bands, lithium dimer diffuse band at 458 nm and the interference continuum at 452 nm are indicated by arrows. The lithium atomic 4^2D-2^2P line is out of scale.

Figures 1a), b), c) show the violet $3^2\Sigma^+$-$1^2\Sigma^+$ bands of LiAr (414 nm), LiKr (420 nm) and LiXe (435 nm), for excitation at 308 nm. The temperature was $T = 1161$ K, yielding a partial lithium vapor pressure of 9 Torr and a density of Li atoms of $7.5 \cdot 10^{16}$ cm^{-3} and a Li_2 partial vapor pressure of 0.5 Torr and Li_2 density of $3.83 \cdot 10^{15}$ cm^{-3}, according to the Nesmeyanov tables [19] and the ideal-gas law. Argon, krypton and xenon pressures were 150, 300 and 200 Torr, respectively. On all three spectra, lithium atomic lines were observed at 413.3 nm (5^2D-2^2P) and 460.3 nm (4^2D-2^2P) and their intensities decreased at higher rare-gas pressure in the heat-pipe oven. We also observed the Li_2 diffuse band at 458 nm ($2^3\Pi_g$-$1^3\Sigma_u^+$) and the interference continuum at 452 nm ($2^1\Sigma_u^+$-$1(X)^1\Sigma_g^+$), as indicated by vertical arrows [20].

Intensities of the LiRG, Li_2 diffuse band and Li_2 interference continuum show an interesting dependence on the rare-gas pressure. These intensities are determined as areas under the observed bands. The Li_2 interference con-

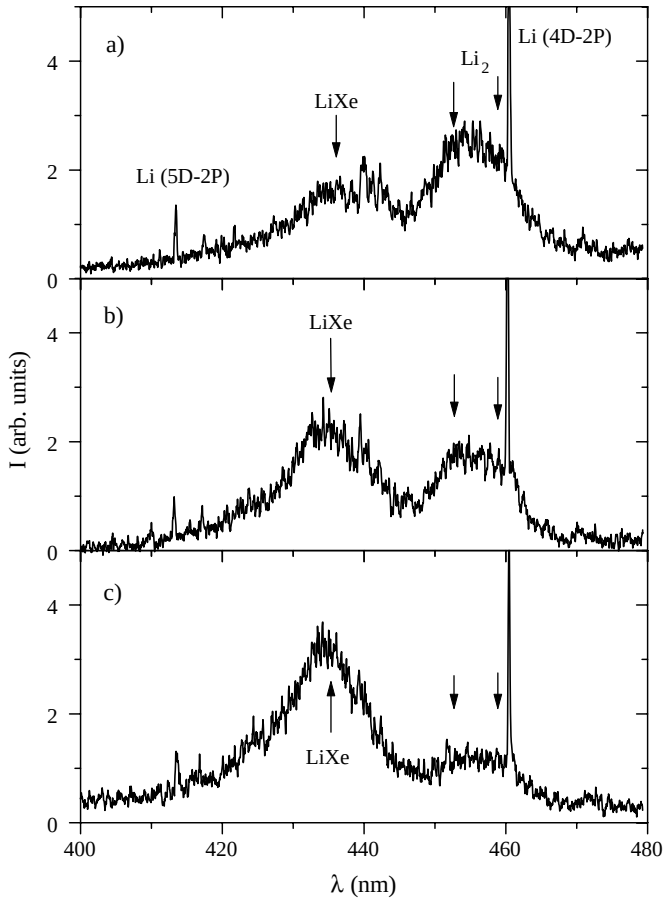

Fig. 2. Dependence of the LiXe band and Li_2 band shapes and intensities on the xenon pressure: a) P_{Xe}=50 Torr, b) P_{Xe}=100 Torr, and c) P_{Xe}=246 Torr. Temperature is 1161 K. Bars indicate the positions of the LiXe band and Li_2 bands.

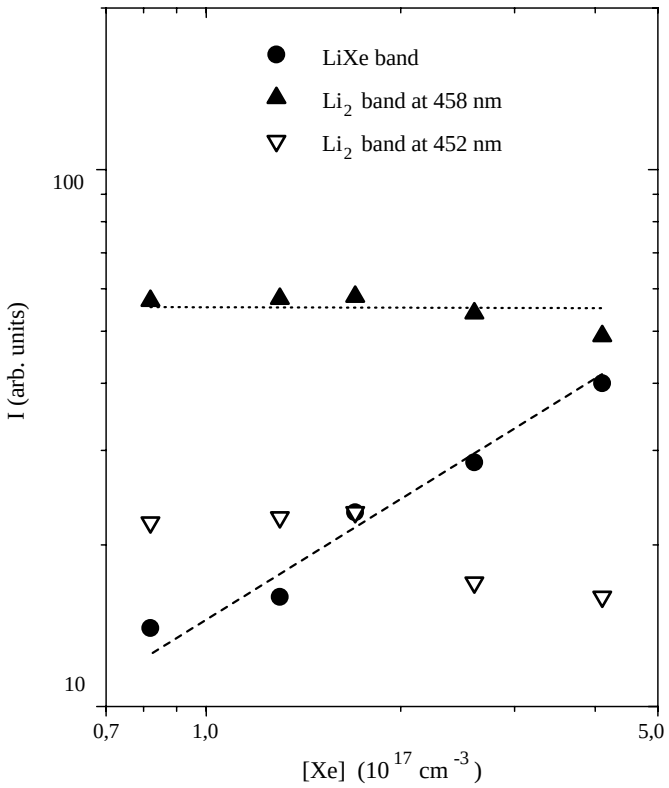

Fig. 3. Intensities of the LiXe band, Li_2 diffuse band and Li_2 interference continuum *versus* the atom density of xenon. The intensities are the areas under the bands and the errors of intensities are up to 20% for Li_2 bands and up to 10% for the LiXe band.

tinuum at 452 nm and the diffuse band at 458 nm overlap and we first obtained the area under both bands together. The intensity of the Li_2 diffuse band was estimated from the intensity at its maximum (458 nm) and its half width, which is about 8 nm and does not change with rare-gas pressure [20]. The interference continuum intensity is then the total intensity minus the diffuse band intensity.

As an example, Figures 2a), b), c) show the LiXe band behavior with increasing xenon pressure for 50, 100 and 246 Torr, respectively. Comparison of the relative intensities of LiXe and Li_2 continuum bands *versus* Xe densities is shown in Figure 3. We compare the photochemical reaction of Li_2 with Xe (see Eq. (1)) with the collisional transfer of population resulting in the Li_2 diffuse band at 458 nm:

$$\mathrm{Li_2}(2(C)^1\Pi_u) + \mathrm{RG} \rightarrow \mathrm{Li_2}(2^2\Pi) + \mathrm{Li}\,. \qquad (2)$$

By inspection of Figure 3 we observe a slight decrease in the intensity at 452 nm, which indicates a small contribution of $Li_2(2^1\Sigma_u^+)$ +Xe $\rightarrow$ LiXe($3^2\Sigma^+$)+Li reaction. However, in all subsequent analysis we shall not take into account this reaction.

The photochemical reaction rate constant k_{LiRG} giving LiRG* can be evaluated from

$$k_{\mathrm{LiRG}} = \frac{\nu_{\mathrm{diff}}}{\nu_{\mathrm{LiRG}}}\frac{\alpha(\nu_{\mathrm{diff}})}{\alpha(\nu_{\mathrm{LiRG}})}\frac{I_{\mathrm{LiRG}}}{I_{\mathrm{diff}}}\frac{\gamma_{\mathrm{LiRG}}}{\gamma_{\mathrm{diff}}}\frac{\Gamma_{\mathrm{diff}}}{\Gamma_{\mathrm{LiRG}}}\frac{[\mathrm{Li}]}{[\mathrm{RG}]}k_{\mathrm{diff}}\,, \quad (3)$$

where ν_{diff}, ν_{LiRG}, $\alpha(\nu_{\mathrm{diff}})$, $\alpha(\nu_{\mathrm{LiRG}})$, I_{LiRG}, I_{diff}, Γ_{diff}, Γ_{LiRG} are frequencies, spectral responses, intensities at the band maxima and radiative transition rates for the given transitions as given in more details in reference [21]. Note that in reference [21] (Eq. (12)) a similar expression is given for the corresponding cross-section $\sigma(\mathrm{cm}^2)$. All these values can be taken from the observed spectrum. The values γ_{LiRG} and γ_{diff} are

$$\gamma_{\mathrm{LiRG}} = \Gamma_{3^2\Sigma^+-1^2\Sigma^+} + \Gamma_{3^2\Sigma^+-2^2\Sigma^+} + \Gamma_{3^2\Sigma^+-1^2\Pi}\,,$$
$$\gamma_{\mathrm{diff}} = \Gamma_{2^3\Pi-1^3\Sigma_u^+} + \Gamma_{2^3\Pi-2^3\Sigma_u^+} + \Gamma_{2^3\Pi-3^3\Sigma_u^+} + \Gamma_{2^3\Pi-1^3\Pi}\,,$$

where diff $\equiv 2^3\Pi - 1^3\Sigma_u^+$ and LiRG $\equiv 3^2\Sigma^+ - 1^2\Sigma^+$. The factor $\gamma_{\mathrm{LiRG}}/\gamma_{\mathrm{diff}}$ can be estimated from the values of transition dipole moments for transitions from the LiRG $3^2\Sigma^+$ state to all radiatively coupled lower states [13] and the values of transition dipole moments for transitions from the Li_2 $2^3\Pi_g$ state to all radiatively coupled lower states [22]. For LiAr this factor is 8.6 and for LiKr and LiXe we could not find any calculated value. Therefore, we assume in the first approximation the same value of 8.6

also for LiKr and LiXe. The factor [Li]/[RG] is the atom density ratio of lithium and rare gas. The rate constant for collisional energy transfer (2) giving the Li_2 diffuse band at 458 nm as obtained by Weyh *et al.* [23] is

$$k_{\rm diff} = \langle \sigma_{\rm diff} v({\rm Li}_2, {\rm Li}) \rangle = (25 \pm 7) \cdot 10^{-16} (8{\rm kT}/\pi\mu)^{1/2} = (5.7 \pm 1.6) \cdot 10^{-10} {\rm cm}^3{\rm s}^{-1}. \quad (4)$$

The intensities of the LiXe band and Li_2 diffuse band and atom densities of Li and Xe from the graph in Figure 3 give $k_{\rm LiXe} = (19 \pm 9) \cdot 10^{-10}$ cm^{3}s^{-1}, using the least square fit method.

Using the same method we obtain rate constants for photochemical formation of LiAr and LiKr in the $3^2\Sigma^+$ state, which are $k_{\rm LiAr} = (2.3 \pm 1.1) \cdot 10^{-10}$ cm^{3}s^{-1} and $k_{\rm LiKr} = (6.9 \pm 3.2) \cdot 10^{-10}$cm^{3}s^{-1}. The ratios of the rate constants for LiRG ($3^2\Sigma^+$) and $Li_2(2^3\Pi_g)$ formation are $k_{\rm LiAr}/k_{\rm diff} = 0.4$, $k_{\rm LiKr}/k_{\rm diff} = 1.21$ and $k_{\rm LiXe}/k_{\rm diff} = 3.33$.

The $k_{\rm LiRG}$ values from LiAr to LiXe increase by a factor of about 8, which implies that, for the heavier rare-gas atom with deeper potential well of the relevant $3^2\Sigma^+$ state, *i.e.* larger energy difference between the Li_2^* energy level and the minimum of the $3^2\Sigma^+$ state potential, the probability of the photochemical reaction (1) rapidly increases, as compared to competitive collisional transfer processes between the excited states of alkali dimers (2).

3.2 Dye laser excitation

The PTP dye laser covers the range from 330 nm to 350 nm. This wavelength range enabled us to excite the $Li_2(2(C)^1\Pi_u)$ levels up to $v' = 6$, which has the energy of 23660 cm^{-1}. There is no evidence in the spectrum around the laser line that we have excited any level in the inner well of the double minimum Li_2 $2^1\Sigma_u^+$ state, below the potential barrier [24]. In order to study the dependence of the LiKr band intensity on the exciting laser wavelength we measured the selected wavelength, excitation spectrum. Figure 4 presents the selected wavelength excitation spectrum taken at the LiKr band maximum (420 nm). The laser wavelength was scanned from 335.2 to 335.4 nm. For large Franck-Condon factors in the Li_2 $1(X)^1\Sigma_g^+ \rightarrow 2(C)^1\Pi_u$ rovibrational excitation, identified in Figure 4, we get maxima in the LiKr band intensity, which proves the validity of the photochemical reaction (1).

4 Potential-energy curves: The LiKr excimer

We calculated LiKr potential-energy curves for the four lowest states of the $^2\Sigma^+$ symmetry and three of the $^2\Pi$ symmetry by using the MOLCAS2 package [25]. The basis set for Li ($6s4p3d$), was used as in reference [7]. For Kr we used primitive functions ($21s16p10d$) reference [26]. We added additional exponents to this: 0.08 and 0.03 for s type, 0.04 and 0.0165 for p type, 0.229 and 0.0916 for d type functions. These additional exponents were obtained from extrapolation of the s and p exponents in a log plot. For d-type functions the exponents were taken

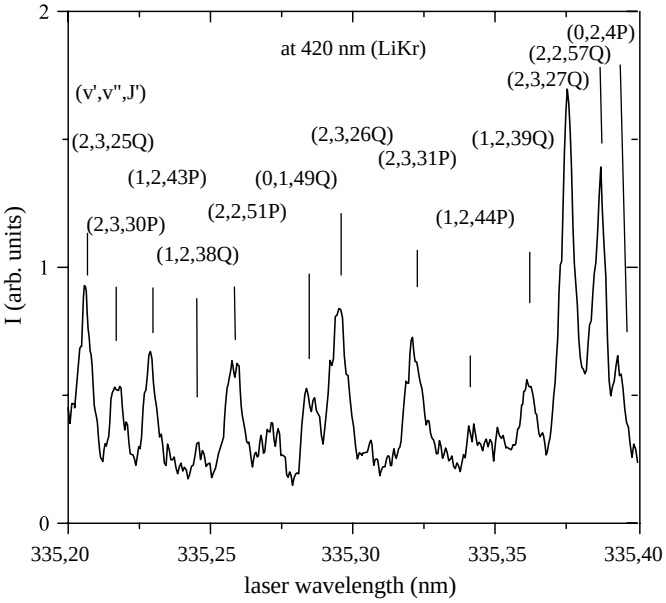

Fig. 4. Selective absorption spectrum on the LiKr excimer band maximum at 420 nm. The maxima correspond to the Li_2 $2^1\Pi_u$-$1^1\Sigma_g^+$ rovibrational transitions (v', v'', J'), identified using spectroscopic constants for the Li_2 $2^1\Pi_u$ and $1^1\Sigma_g^+$ states [29–31].

from reference [27]. As in reference [27] even-tempered $4f$ type exponents were added. With this basis set almost the complete Hartree-Fock total energy was obtained at -2752.051 Hartree [28]. Spherical coordinates were used giving with the above basis set 210 primitives and 81 contracted basis functions. The calculation was performed in the C_{2v} symmetry. In MRCI 28 electrons were frozen (7,3,3,1) in $a1$, $b1$, $b2$, $a2$ irreducible representations and 22 virtual orbitals were deleted (12,5,5,0). In MRCI calculations 11 electrons were correlated ($1s$ and $2s$ of Li and $4s$ and $4p$ of Kr). Nine main references were used defining a real space of 51709 configurations. Prior to the MRCI either a SCF or a CASSCF calculations were performed. First order relativistic corrections (mass-velocity and Darwin term) were included as well [25].

Table 1 presents the *ab initio* potential energies for the LiKr $1^2\Sigma^+$, $2^2\Sigma^+$, $3^2\Sigma^+$, $4^2\Sigma^+$, $1^2\Pi$, $2^2\Pi$ and $3^2\Pi$ states. In Table 2 we give dipole moment for the ground state and transition dipole moments for the LiKr Σ-Σ transitions. Note that values and dependence on R obtained for LiKr molecule are similar to those of LiAr [13, 14] which supports our assumptions in Section 3.1. Table 3 presents the spectroscopic constants for the LiKr $1^2\Sigma^+$, $1^2\Pi$, $2^2\Sigma^+$, $3^2\Sigma^+$ and $2^2\Pi$ states. Table 4 presents a comparison of the R_e and T_e taken from the LiKr $1^2\Sigma^+$ and $1^2\Pi$ *ab initio* potentials with the values calculated by Pascale and Vandeplanque [11] and with the experimental values given by Auerbach [17] and Scheps *et al.* [18]. From these data, we may conclude that the *ab initio* calculation of the ground state gives too deep minimum, because the experimental value is about 70 cm^{-1}. We believe that this is mainly due to the basis set superposition error. However, the difference potentials relevant to spectroscopy should be more accurate.

Table 1. Potential energies for LiKr molecule in hartree, interatomic separation R is in bohr.

R	$1^2\Sigma^+$	$2^2\Sigma^+$	$3^2\Sigma^+$	$4^2\Sigma^+$	$1^2\Pi$	$2^2\Pi$	$3^2\Pi$
3.25	−0.4005085	−0.3234644	−0.2961731	−0.2876754	−0.3380897	−0.2920849	−0.2772029
3.5	−0.4375632	−0.3612275	−0.3339143	−0.3248739	−0.3780887	−0.3292013	−0.3156819
3.75	−0.4596559	−0.3832798	−0.3561417	−0.3465490	−0.4021021	−0.3505374	−0.3382916
4.	−0.4726528	−0.3956805	−0.3688309	−0.3585256	−0.4161919	−0.3621480	−0.3510792
4.25	−0.4801896	−0.4022790	−0.3757338	−0.3645550			
4.5	−0.4844912	−0.4055250	−0.3791750	−0.3670242	−0.4283643	−0.3697614	−0.3611132
5.	−0.4883810	−0.4080389	−0.3809768	−03667541	−0.4310826	−0.3689544	−0.3618997
5.5	−0.4897088	−0.4095498	−0.3796883	−0.3641447	−0.4303854	−0.3653886	−0.3595355
6.	−0.4903606	−0.4121060	−0.3774106	−0.3602489	−04289024	−0.3617274	−0.3567152
7.	−0.4911732	−0.4165793	−0.3728927	−0.3552986	−0.4263529	−0.3564139	−0.3523502
8.					−0.4251961	−0.3541763	−0.3507252
8.5	−0.4920470	−0.4216463	−0.3701660	−0.3536025			
9.5					−0.4248510	−0.3532627	−0.3505684
10.	−0.4923555	−0.4237854	−0.3696169	−0.3531456			
11.	−0.4921555	−0.4240683	−0.3693427	−0.3526411	−0.4244894	−0.3527058	−0.3505085
12.5	−0.4919990	−0.4239981	−0.3693398	−0.3523484			
15.	−0.4920005	−0.4240205	−0.3696144	−0.3522318	−0.4242991	−0.3524386	−0.3505300
18.	−0.4918726	−0.4238290	−0.3695808	−0.3522761	−0.4241580	−0.3522776	−0.3504068

Table 2. Dipole moment for the ground state and transition dipole moments for LiKr in atomic units.

R	$1^2\Sigma^+$	$2^2\Sigma^+$-$1^2\Sigma^+$	$3^2\Sigma^+$-$1^2\Sigma^+$	$4^2\Sigma^+$-$1^2\Sigma^+$
3.25	1.77776874	1.86186478	0.92245651	0.38236908
3.5	1.79671425	1.90200787	0.91466456	0.36047910
3.75	1.79152689	1.93262393	0.90494948	0.33517901
4	1.76002886	1.96183103	0.89052320	0.30862715
4.25	1.70208274	1.99678065	0.86668951	0.28140826
4.5	1.61937599	2.04227469	0.82738405	0.25065849
5	1.40927266	2.12598452	0.69529641	0.24336991
5.5	1.14072158	2.25505190	0.50135385	0.23199599
6	0.87099314	2.33929207	0.29932825	0.17813524
7	0.42212540	2.38938202	0.06776487	0.03502065
8.5	0.12787435	2.41388895	0.00413534	0.03975754
10	0.03951016	2.41989614	0.00830578	0.06651151
11	0.02049474	2.41730242	0.00368579	0.06967306
12.5	0.01641412	2.41121085	0.00348032	0.06437032
15	0.01526793	2.39976461	0.00479587	0.07530521
18	0.01638541	2.39239426	0.00267635	0.08321014

Table 3. Calculated spectroscopic constants of LiKr (in cm^{-1}).

State	R_e(bohr)	D_e	T_e	B_e	ω_e	$\omega_e x_e$	α_e	$v_{\max}$	$E_{\exp}(\infty)$
$1^2\Sigma^+$	9.36	273	-273	0.105	9.9	0.85	0.012	5	0
$1^2\Pi$	5.06	1411	13444	0.362	218.4	9.1	0.003	11	14855
$2^2\Sigma^+$	11.71	88	14767	0.068	4212	4.3	0.005	4	14855
$3^2\Sigma^+$	4.95	2509	24395	0.373	229.1	5.1	0.005	22	26904
$2^2\Pi$	4.64	3806	26849	0.431	313.7	6.7	0.011	22	30655

Table 4. Comparison of the LiKr $1^2\Sigma^+$ and $1^2\Pi$ excited states with the previously published experimental [18,17] and calculated potentials [11].

State	Reference	R_e(bohr)	T_e(cm^{-1})
$1^2\Sigma^+$	This work	9.36	−273
	Auerbach [17]	9.04	−67.9
	Pascale *et al.* [11]	9.45	−65.7
$1^2\Pi$	This work	5.06	13444
	Scheps *et al.* [18]	6.01	13800
	Pascale *et al.* [11]	6.0	14300

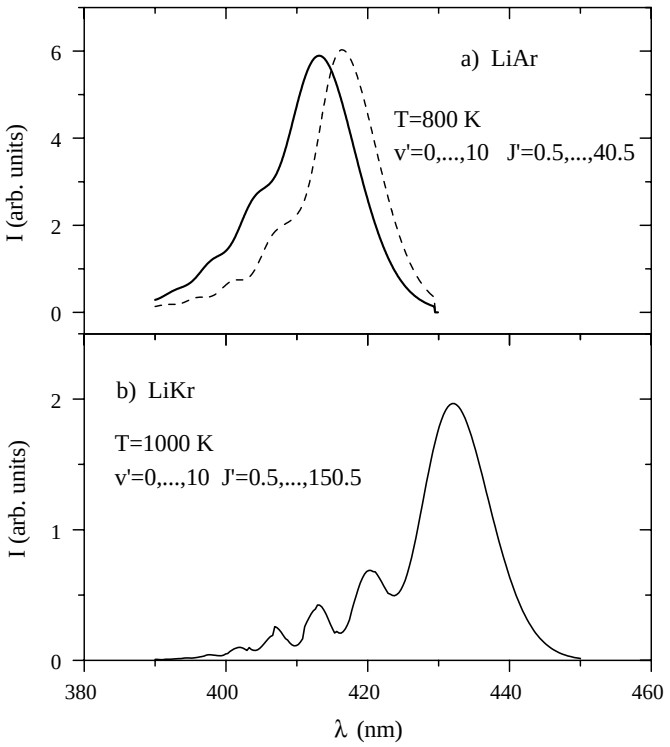

Fig. 5. a) Spectral simulation of the LiAr $3^2\Sigma^+$-$1^2\Sigma^+$ transition using the *ab initio* potential-energy curves from reference [13] (dashed line) and reference [14] (full line). b) Spectral simulation of the LiKr $3^2\Sigma^+$-$1^2\Sigma^+$ transition using the *ab initio* potential-energy curves from Section 4.

5 Spectral simulation of the LiAr and LiKr $3^2\Sigma^+$-$1^2\Sigma^+$ bands

Ab initio potential-energy curves, transition dipole moments and spectroscopic constants for LiAr are published by Gu *et al.* [13] and Park *et al.* [14]. The *ab initio* LiAr ground-state potential given in reference [13] is completely repulsive whereas calculation of reference [14] shows shallow minimum at about 10 Bohr, closer to the experimental values [15,16]. The $3^2\Sigma^+$ state has a shallow minimum and contains only 10 bound vibrational levels for $J' = 25.5$. Note that the shallow outer well of the $3^2\Sigma^+$ potential, which is obtained in calculation of reference [14], does not affect spectral formation of the considered LiAr diffuse band. We performed the quantum mechanical simulation using the standard Numerov-Cooley method for the bound-free transitions [32]. Rotational averaging was performed over $J' = 0.5$-40.5, assuming a Boltzmann distribution. The rovibrationally averaged LiAr spectral simulations for the effective temperature of 800 K are given in Figure 5a). The calculated peak position is at 416.4 nm using potentials from reference [13] and 413.1 nm using potentials from reference [14], which is in good agreement with the measured peak position at 414 nm.

Table 5. Maxima (λ) of the LiAr, LiKr and LiXe excimer bands compared with the observations (λ^*) of Wang and Havey [6] and the calculations (λ^c).

	LiAr	LiKr	LiXe
λ(nm)	414	420	435
λ^*(nm)	411	416	431
λ^c(nm)	416.4 [a]	433	
	413.1 [b]		

[a] Using reference [13].
[b] Using reference [14].

Prior to this simulations we performed another spectral simulation of the LiAr $3^2\Sigma^+$-$1^2\Sigma^+$ transition using a different set of the *ab initio* potential energy curves and transition dipole moments as reported in reference [33]. The calculated maximum of the LiAr band was at 405 nm. The shape of the simulated LiAr band was similarly asymmetric as in Figure 5a) but without the quantum oscillations on the blue wing of the band.

Using the potential-energy curves given in Table 1, transition dipole moments given in Table 2 and spectroscopic constants given in Table 3, we performed quantum-mechanical spectral simulations of the LiKr $3^2\Sigma^+$-$1^2\Sigma^+$ band. The emission profiles for the range of rotational numbers from 0.5 to 150.5 and vibrational numbers from 0 to 10 were obtained in which the rotational averaging assuming the Boltzmann distribution for an effective temperature of 1000 K was assumed. The rotationally averaged spectra are vibrationally averaged assuming the Boltzmann distribution among 11 vibrational levels which give a significant contribution to the spectrum. Figure 5b) shows simulation of the LiKr $3^2\Sigma^+$-$1^2\Sigma^+$ band with the maximum at 433 nm, which is shifted by 710 cm^{-1} from the experimental position at 420 nm. Table 5 gives the experimental positions of LiAr, LiKr and LiXe bands observed in this work and in the work of Wang and Havey, as well as the calculated positions of the LiAr and LiKr excimer bands.

6 Discussion

First we present the systematization of the possible photochemical reactions populating LiAr and LiKr in their excited states. Table 6 presents a list of possible photochemical reactions populating the LiAr (upper part) and LiKr (lower part) excited states. We give the energy defect, and the positions of extrema in the difference potentials of the

Table 6. A list of photochemical reactions producing the excited LiAr and LiKr excimers. We give the energy defect of the reaction, the spectral positions of the listed transitions calculated from the extrema in difference potentials and observed values (in nm), where available.

Reaction	$\Delta E\,(\mathrm{cm}^{-1})$	Transition	Calculated position in nm, comments
$Li(2^2P)+Ar+Ar \rightarrow LiAr(1^2\Pi)+Ar$	79	$1^2\Pi \rightarrow 1^2\Sigma^+$	674, min at 4.2 bohr, obs. at 790 [18]
$Li_2(1^1\Sigma_u^+)+Ar \rightarrow LiAr(1^2\Pi)+Li$	−9270	$1^2\Pi \rightarrow 1^2\Sigma^+$	674, min at 4.2 bohr, obs. at 740 [10]
$Li_2(1^1\Pi_u)+Ar \rightarrow LiAr(1^2\Pi)+Li$	−2902		
$Li(3^2P)+Ar+Ar \rightarrow LiAr(3^2\Sigma)+Ar$	4807	$3^2\Sigma^+ \rightarrow 1^2\Sigma^+$	416, min at 3.5 bohr, obs. at 411 [6]
$Li(3^2D)+Ar+Ar \rightarrow LiAr(3^2\Sigma)+Ar$	5166		
$Li(3^2P)+Ar+Ar \rightarrow LiAr(2^2\Pi)+Ar$	1837	$2^2\Pi \rightarrow 1^2\Sigma^+$	394, min at 3.5 bohr, obs. at 380 [6]
$Li(3^2D)+Ar+Ar \rightarrow LiAr(2^2\Pi)+Ar$	2196		
$Li_2(2^1\Pi_u)+Ar \rightarrow LiAr(3^2\Sigma)+Li$	−4064	$3\ ^2\Sigma^+ \rightarrow 1^2\Sigma^+$	416, min at 3.5 bohr
$Li_2(2^1\Sigma_u^+)+Ar \rightarrow LiAr(3^2\Sigma)+Li$	−4315	$3^2\Sigma^+ \rightarrow 1^2\Pi$	825, max at 5.2 bohr
		$3^2\Sigma^+ \rightarrow 2^2\Sigma^+$	1674, min at 4 bohr
$Li_2(2^1\Pi_u)+Ar \rightarrow LiAr(2^2\Pi)+Li$	−7034	$2^2\Pi \rightarrow 1^2\Sigma^+$	394, min at 3.5 bohr
$Li_2(2^1\Sigma_u^+)+Ar \rightarrow LiAr(2^2\Pi)+Li$	−7285	$2^2\Pi \rightarrow 1^2\Pi$	no extrema
		$2^2\Pi \rightarrow 2^2\Sigma^+$	631, max at 14 bohr
$Li(2^2P)+Kr+Kr \rightarrow LiKr(1^2\Pi)+Kr$	1559	$1^2\Pi \rightarrow 1^2\Sigma^+$	744, min at 4.5 bohr, obs. at 802 [18]
$Li_2(1^1\Sigma_u^+)+Kr \rightarrow LiKr(1^2\Pi)+Li$	−7876	$1^2\Pi \rightarrow 1^2\Sigma^+$	744, min at 4.5 bohr
$Li_2(1^1\Pi_u)+Kr \rightarrow LiKr(1^2\Pi)+Li$	−1508		
$Li(3^2P)+Kr+Kr \rightarrow LiKr(3^2\Sigma)+Kr$	6539	$3^2\Sigma^+ \rightarrow 1^2\Sigma^+$	433, min at 3.5 bohr, obs. at 416 [6]
$Li(3^2D)+Kr+Kr \rightarrow LiKr(3^2\Sigma)+Kr$	6898		
$Li(3^2P)+Kr+Kr \rightarrow LiKr(2^2\Pi)+Kr$	4085	$2^2\Pi \rightarrow 1^2\Sigma^+$	401, min at 3.5 bohr, obs. at 392 [6]
$Li(3^2D)+Kr+Kr \rightarrow LiKr(2^2\Pi)+Kr$	4444		
$Li_2(2^1\Pi_u)+Kr \rightarrow LiKr(3^2\Sigma)+Li$	−2332	$3\ ^2\Sigma^+ \rightarrow 1^2\Sigma^+$	433, min at 3.5 bohr
$Li_2(2^1\Sigma_u^+)+Kr \rightarrow LiKr(3^2\Sigma)+Li$	−2583	$3^2\Sigma^+ \rightarrow 1^2\Pi$	1053, min at 4 bohr
		$3^2\Sigma^+ \rightarrow 2^2\Sigma^+$	1904, min at 4.7 bohr
$Li_2(2^1\Pi_u)+Kr \rightarrow LiKr(2^2\Pi)+Li$	−4786	$2^2\Pi \rightarrow 1^2\Sigma^+$	401, min at 3.5 bohr
$Li_2(2^1\Sigma_u^+)+Kr \rightarrow LiKr(2^2\Pi)+Li$	−5037	$2^2\Pi \rightarrow 1^2\Pi$	no extrema
		$2^2\Pi \rightarrow 2^2\Sigma^+$	1324, min at 4.5 bohr

excited LiAr (LiKr) product of the reaction, and the spectral position of the observed bands. Because of the shallow minima of the LiAr excited states, usually we have to excite very high rovibrational levels in the Li_2 excited states. The other way of LiAr* formation is through the three-body recombination. These reactions are presented as collisions of Li atom in the excited state with two Ar atoms, giving LiAr in the excited state and the other argon atom in the ground state. Such collisions were studied in several papers. Excitation of the LiAr $1^2\Pi$ state by exciting the lithium atomic 2^2P state was studied by Scheps *et al.* [18]. The formation of the LiAr $3^2\Sigma^+$ and $2^2\Pi$ states by exciting lithium to 3^2P and 3^2D levels was studied by Wang and Havey [6]. In the work of Zhang and Ma, the lithium dimer was excited by a He-Ne laser to the high rovibrational levels of the Li_2 $1(A)^1\Sigma_u^+$ state and they observed the photochemical reaction leading to the LiAr $1^2\Pi$ state [10]. Other photochemical reactions listed in Table 6 were not studied up to now.

Collisions of one lithium atom in an excited state with two Kr atoms are the only three-body recombinations observed so far. Excitation of the lithium resonance line gives the LiKr band at 801 nm [18]. Wang and Havey studied the excitation of lithium 3^2P and 3^2D states, populating the LiKr $3^2\Sigma^+$-$1^2\Sigma^+$ states [6]. Photochemical reactions from the lithium dimer states, as the input channel, to the LiKr excited states, as the output channel, have not been observed to date.

The observation of the relatively intensive LiRG $3^2\Sigma^+$-$1^2\Sigma^+$ bands can be explained by analyzing the shape of the potential-energy curves of Li_2 and LiRG, which are presented in Figures 6a) and b), respectively. The $2^2\Sigma^+$ state is repulsive, with a shallow van der Waals well at large internuclear separations. Such a repulsive $2^2\Sigma^+$ state has an avoided crossing with an energetically higher $3^2\Sigma^+$ state, which has the same symmetry. This avoided crossing is responsible for the increase of the transition dipole moment of the $3^2\Sigma^+$-$1^2\Sigma^+$ transition (intensity borrowing). The $2^2\Pi$ states in alkali–rare-gas excimers does not over-

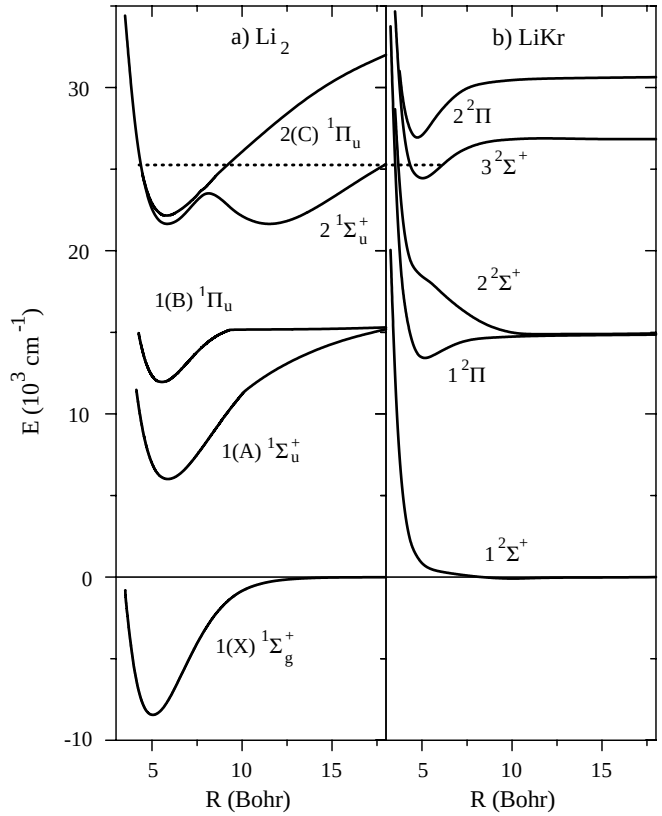

Fig. 6. a) The Li_2 $1^1\Sigma_g^+$, $1^1\Sigma_u^+$, $1^1\Pi_u$, $2^1\Sigma_u^+$ and $2^1\Pi_u$ potentials [29–31]. b) *Ab initio* potential-energy curves of the LiKr excimer.

lap with the $3^2\Sigma^+$ state and the transition dipole moment for the $2^2\Pi$-$1^2\Sigma^+$ transition is about 3 times lower than that for the $3^2\Sigma^+$-$1^2\Sigma^+$ transition. Photochemical population of the $3^2\Sigma^+$ state is preferred here, since for the photochemical population of the $2^2\Pi$ state more energy is needed for excited alkali dimers in the input channel of the reaction. The $2^2\Pi$ state can be achieved in three atom collisions, including the alkali atom in the second excited P state or the first excited D state with two rare-gas atoms. Because of the shallow $3^2\Sigma^+$ states in LiRG excimers, the higher laser photon energies are more probable to populate the LiRG $3^2\Sigma^+$ state in reaction (1). Therefore the excimer laser line at 308 nm gives more intensive LiRG bands than the dye laser excitation at photon energies of 335 nm. The smallest excitation energy in the $Li_2\,2(C)^1\Pi_u$ state which will enable photochemical formation of the $3^2\Sigma^+$ state is 25544 cm^{-1} and 24395 cm^{-1} for LiAr and LiKr, respectively. According to Table 5 the calculated LiKr excited states are too deep by about 500 cm^{-1}, which moves T_e(LiKr) to 24900 cm^{-1}. The excimer laser line at 308 nm which populates $Li_2(2(C)^1\Pi_u)$ with $E = 26260.7\,cm^{-1}$ provides for all LiGR molecules enough energy to start reaction (1). In the case of dye laser excitation at 335 nm, $E = 23660\ cm^{-1}$ does not reach the threshold for the reaction (1) for LiAr and LiKr. However, we observe the reaction at high-temperature and rare-gas pressure because the collisional energies give an additional 1000 cm^{-1}. The positions of maxima of the LiRG bands at 414, 420 and 435 nm correspond to energies of 24154, 23809 and 22988 cm^{-1} for LiAr, LiKr and LiXe, respectively. Spectral simulations give maxima in the LiAr and LiKr bands at 416 and 433 nm, which correspond to energies of 24038 and 23095 cm^{-1}, respectively. Using all these values we can roughly estimate the error of the $3^2\Sigma^+$-$1^2\Sigma^+$ difference potential, which is about 120 cm^{-1} for LiAr and 700 cm^{-1} for LiKr.

The large uncertainties in the determination of the rate constants k_{LiRG}, which are about 50%, are mainly due to the uncertainty of the collisional energy transfer cross-section σ_{diff} [23], which is 28%. The second large contribution is the uncertainty in the intensity measurements of the Li_2 diffuse band at 458 nm, which is about 15% because of the overlap with the Li_2 interference continuum at 452 nm. The LiRG bands are not disturbed by other molecular transitions and the error in the intensity determination is not higher than 5%. The errors in the atom density ratios [RG]/[Li], frequencies and spectral responses are not larger than few %. The accuracy of the factor $\gamma_{\mathrm{LiRG}}\ /\gamma_{\mathrm{diff}}$ for LiAr depends on the uncertainties of transition dipole moments. For LiKr and LiXe we took the same value as for LiAr and, in these cases, rate constants may be underestimated since the transition dipole moments for LiKr and LiXe are slightly larger than for LiAr.

7 Conclusion

We investigated photochemical formation of the lithium–rare-gas $3^2\Sigma^+$ states in the reaction given by relation (1). We worked with all rare gases, from He to Xe, but we observed no LiHe and LiNe $3^2\Sigma^+$-$1^2\Sigma^+$ bands in the spectrum. The LiAr, LiKr and LiXe $3^2\Sigma^+$-$1^2\Sigma^+$ transitions were observed at 414, 420 and 435 nm, respectively. We found that the rare-gas pressure had to be at least about 2 times larger than the lithium vapor pressure if we want to observe the LiRG band as a result of the above reaction. We estimated rate constants for this photochemical reaction at $T = 1160$ K as $(2.3 \pm 1.1) \cdot 10^{-10}$ cm^3s^{-1}, $(6.9 \pm 3.2) \cdot 10^{-10}$ cm^3s^{-1} and $(19 \pm 9) \cdot 10^{-10}$ cm^3s^{-1} for LiAr, LiKr and LiXe, respectively, measured relatively to the collisional energy transfer [23]. The photochemical reaction can populate only the $3^2\Sigma^+$ state of the Li–rare-gas excimer because the $2^2\Pi$ state is energetically too high. Spectral simulations of the LiAr and LiKr $3^2\Sigma^+$-$1^2\Sigma^+$ transitions were calculated using the recently calculated *ab initio* potential-energy curves. Using potentials of reference [14] spectral simulation of the LiAr band gives peak at 413.1 nm, in better agreement with experimental position at 414 nm, compared to the case when using potentials of reference [13]. The simulated position of the LiKr band is at 433 nm. It is shifted by about 13 nm to the red, as compared with the experimental value of 420 nm. The LiKr ground state *ab initio* potential is about 200 cm^{-1} too deep when compared with the experimental potential. To reproduce the experimental position of the LiKr band,

we have to add about 800 cm^{-1} to the $3^2\Sigma^+$ *ab initio* potential.

This work was financially supported by the Ministry of Science and Technology of the Republic of Croatia. We also gratefully acknowledge partial support from the Alexander von Humboldt Stiftung, Germany. One of us (S.M.) is grateful to the Max-Planck-Institut für Strömungsforschung for the hospitality during his stay in Göttingen.

References

1. F. Rostas, *Alkali-rare gas excimers,* in *Spectral line shapes*, Vol. I (Walter de Gruyter, Berlin, New York, 1981), p. 767.
2. A.C. Tam, G. Moe, W. Park, W. Happer, Phys. Rev. Lett. **35**, 85 (1975).
3. A.C. Tam, G. Moe, B.R. Bulos, W. Happer, Opt. Commun. **16**, 376 (1976).
4. A.C. Tam, G. Moe, Phys. Rev. A **14**, 528 (1976).
5. Ch.R. Webster, F. Rostas, Chem. Phys. Lett. **59**, 57 (1978).
6. W.J. Wang, M.D. Havey, Phys. Rev. A **29**, 3184 (1984).
7. S. Milošević, X. Li, D. Azinović, G. Pichler, M.C. van Hemert, A. Stehouwer, R. Düren, J. Chem. Phys. **96**, 7364 (1992).
8. M.C. van Hemert, D. Azinović, X. Li, S. Milošević, G. Pichler, R. Düren, Chem. Phys. Lett. **200**, 97 (1992).
9. D. Azinović, X. Li, S. Milošević, G. Pichler, M.C. van Hemert, R. Düren, J. Chem. Phys. **98**, 4672 (1993).
10. L-M. Zhang and X-X. Ma, Opt. Commun. **83**, 310 (1991).
11. J. Pascale, J. Vandeplanque, J. Chem. Phys. **60**, 2278 (1974).
12. M. Jungen, V. Stäumler, J. Phys. B: At. Mol. Opt. Phys. **21**, 463 (1988).
13. J.-P. Gu, G. Hirsch, R.J. Buenker, I.D. Petsalakis, G. Theodorakopoulos, M.-B. Huang, Chem. Phys. Lett. **230**, 473 (1994).
14. J. Park, Y.S. Lee, G.-Hi Jeung, Chem. Phys. Lett. **277**, 208 (1997).
15. U. Buck, H. Pauly, Z. Phys. **208**, 390 (1968).
16. R. Brühl, D. Zimmermann, Chem. Phys. Lett. **233**, 455 (1995).
17. D.J. Auerbach, J. Chem. Phys. **60**, 4116 (1974).
18. R. Scheps, Ch. Ottinger, G. York, A. Gallagher, J. Chem. Phys. **63**, 2581 (1975).
19. A.N. Nesmeyanov, *Vapor Pressure for Chemical Elements*, edited by R. Gray (Elsevier, New York, 1963).
20. X. Li, Ph.D. thesis, *Spectroscopic studies of LiLi, LiZn and LiCd molecules in vapor mixtures*, Institute of Physics, Zagreb, Croatia, 1992.
21. D. Azinović, S. Milošević, G. Pichler, Z. Phys. D **36**, 147 (1996).
22. L.B. Ratcliff, J.L. Fish, D.D. Konowalow, J. Mol. Spectrosc. **122**, 293 (1987).
23. Th. Weyh, K. Ahmed, W. Demtröder, Chem. Phys. Lett. **248**, 442 (1996).
24. X. Li, D. Azinović, S. Milošević, G. Pichler, Z. Phys. D **28**, 135 (1993).
25. MOLCAS version 2, K. Anderson, M.P. Füscher, R. Lindh, P.-Å. Malmquist, J. Olson, B.O. Roos, A.J. Sadlej, University of Lund, Sweden, and P.-O. Widmark, IBM Sweden 1991.
26. H. Partridge, J. Chem. Phys. **90**, 1043 (1989).
27. J.E. Rice, P.R. Taylor, T.J. Lee, J. Almlöf, J. Chem. Phys. **94**, 4972 (1991).
28. A. Schäfer, H. Horn, R. Ahlrichs, J. Chem. Phys. **97**, 251 (1992).
29. D.D. Konowalow, J.L. Fish, Chem. Phys. **77**, 435 (1983); *ibid.* **84**, 463 (1984).
30. K. Ishikawa, S. Kubo, H. Kato, J. Chem. Phys. **95**, 8803 (1991).
31. I. Schmidt-Mink, W. Müller, W. Meyer, Chem. Phys. **76**, 4961 (1982); *ibid.* **92**, 263 (1985).
32. B. Numerov, Publs. Observatorie Central Astrophys. Russ. **2**, 188 (1933); J.W. Cooley, Math. Comput. **15**, 363 (1961).
33. D. Azinović, Ph.D. Thesis: *Photochemical formation of alkali-IIB and lithium-rare gas excimers*, Institute of Physics, Zagreb, Croatia, 1994.